

# Background-free fluorescence detection of cold atoms in a two-color magneto-optical trap

Baodong Yang, Qiangbing Liang, Jun He, and Junmin Wang\*

State Key Laboratory of Quantum Optics and Quantum Optics Devices (Shanxi University), and Institute of Opto-Electronics, Shanxi University, Taiyuan 030006, Shanxi Province, China

\*[wwjjmm@sxu.edu.cn](mailto:wwjjmm@sxu.edu.cn)

**Abstract:** A two-color magneto-optical trap (MOT) for trapping cesium (Cs) atoms is experimentally realized. This two-color MOT employs the radiation forces due to photon scattering from the Cs  $6P_{3/2} F' = 5 - 8S_{1/2} F'' = 4$  excited-state transition, which replaced one pair of the three pairs of cooling/trapping laser beams operating on a single-photon red detuning to the Cs  $6S_{1/2} F = 4 - 6P_{3/2} F' = 5$  cycling transition in a standard six-beam Cs MOT, and can cool and trap atoms on both the red-detuning and blue-detuning sides of the two-photon resonance. Employing the two-color MOT, the background-free fluorescence detection of trapped atoms has been demonstrated. This technique will be useful for observation of weak fluorescence signal radiated from single atoms in MOT.

©2012 Optical Society of America

**OCIS codes:** (020.3320) Laser cooling; (190.4180) Multiphoton processes; (270.1670) Coherent optical effects.

---

## References and links

1. E. L. Raab, M. Prentiss, A. Cable, S. Chu, and D. E. Pritchard, "Trapping of neutral sodium atoms with radiation pressure," *Phys. Rev. Lett.* **59**(23), 2631–2634 (1987).
2. C. Monroe, W. Swann, H. Robinson, and C. Wieman, "Very cold trapped atoms in a vapor cell," *Phys. Rev. Lett.* **65**(13), 1571–1574 (1990).
3. J. W. R. Tabosa, G. Chen, Z. Hu, R. B. Lee, and H. J. Kimble, "Nonlinear spectroscopy of cold atoms in a spontaneous-force optical trap," *Phys. Rev. Lett.* **66**(25), 3245–3248 (1991).
4. M. M. Boyd, A. D. Ludlow, S. Blatt, S. M. Foreman, T. Ido, T. Zelevinsky, and J. Ye, " $^{87}\text{Sr}$  lattice clock with inaccuracy below  $10^{-15}$ ," *Phys. Rev. Lett.* **98**(8), 083002 (2007).
5. Z. Hu and H. J. Kimble, "Observation of a single atom in a magneto-optical trap," *Opt. Lett.* **19**(22), 1888–1890 (1994).
6. F. Ruschewitz, D. Bettermann, J. L. Peng, and W. Ertmer, "Statistical investigations on single trapped neutral atoms," *Europhys. Lett.* **34**(9), 651–656 (1996).
7. D. Haubrich, H. Schadowinkel, F. Strauch, B. Ueberholz, R. Wynands, and D. Meschede, "Observation of individual neutral atoms in magnetic and magneto-optical traps," *Europhys. Lett.* **34**(9), 663–668 (1996).
8. W. D. Phillips, "Laser cooling and trapping of neutral atoms," *Rev. Mod. Phys.* **70**(3), 721–741 (1998).
9. S. Wu, T. Plisson, R. C. Brown, W. D. Phillips, and J. V. Porto, "Multiphoton magneto-optical trap," *Phys. Rev. Lett.* **103**(17), 173003 (2009).
10. A. S. Tychkov, J. C. J. Koelemeij, T. Jeltse, W. Hogervorst, and W. Vassen, "Two-color magneto-optical trap for metastable helium," *Phys. Rev. A* **69**(5), 055401 (2004).
11. Q. Cao, X. Y. Luo, K. Y. Gao, X. R. Wang, D. M. Chen, and R. Q. Wang, "Improved atom number with a dual color magneto-optical trap," *Chin. Phys. B* **21**(4), 043203 (2012).
12. R. T. Willis, F. E. Becerra, L. A. Orozco, and S. L. Rolston, "Four-wave mixing in the diamond configuration in an atomic vapor," *Phys. Rev. A* **79**(3), 033814 (2009).
13. F. E. Becerra, R. T. Willis, S. L. Rolston, and L. A. Orozco, "Nondegenerate four-wave mixing in rubidium vapor: the diamond configuration," *Phys. Rev. A* **78**(1), 013834 (2008).
14. D. V. Sheludko, S. C. Bell, R. Anderson, C. S. Hofmann, E. J. D. Vredenberg, and R. E. Scholten, "State-selective imaging of cold atoms," *Phys. Rev. A* **77**(3), 033401 (2008).
15. H. Ohadi, M. Himsforth, A. Xuereb, and T. Freegarde, "Magneto-optical trapping and background-free imaging for atoms near nanostructured surfaces," *Opt. Express* **17**(25), 23003–23009 (2009).
16. B. D. Yang, Q. B. Liang, J. He, T. C. Zhang, and J. M. Wang, "Narrow-linewidth double-resonance optical pumping spectrum due to electromagnetically induced transparency in ladder-type inhomogeneously broadened media," *Phys. Rev. A* **81**(4), 043803 (2010).
17. B. D. Yang, J. Gao, T. C. Zhang, and J. M. Wang, "Electromagnetically induced transparency without a Doppler background in a multilevel ladder-type cesium atomic system," *Phys. Rev. A* **83**(1), 013818 (2011).

18. B. D. Yang, J. Y. Zhao, T. C. Zhang, and J. M. Wang, "Improvement of the spectra signal-to-noise ratio of cesium  $6P_{3/2} - 8S_{1/2}$  transition and its application in laser frequency stabilization," *J. Phys. D Appl. Phys.* **42**(8), 085111 (2009).
19. J. He, B. D. Yang, T. C. Zhang, and J. M. Wang, "Improvement of the signal-to-noise ratio of laser-induced-fluorescence photon-counting signals of single-atoms magneto-optical trap," *J. Phys. D Appl. Phys.* **44**(13), 135102 (2011).
20. T. Liu, T. Geng, S. B. Yan, G. Li, J. Zhang, J. M. Wang, K. C. Peng, and T. C. Zhang, "Characterizing optical dipole trap via fluorescence of trapped cesium atoms," *Sci. China Ser. G* **49**(3), 273–280 (2006).
21. W. Jing, H. Jun, Q. Ying, Y. Bao-Dong, Z. Jiang-Yan, Z. Tian-Cai, and W. Jun-Min, "Observation of single neutral atoms in a large-magnetic-gradient vapor cell magneto-optical trap," *Chin. Phys. B* **17**(6), 2062–2065 (2008).
22. S. V. Kargapol'tsev, V. L. Velichansky, A. V. Yarovitsky, A. V. Taichenachev, and V. I. Yudin, "Optical cascade pumping of the  $7P_{3/2}$  level in cesium atoms," *Quantum Electron.* **35**(7), 591–597 (2005).
23. A. M. Kulshin, A. A. Orel, and R. J. McLean, "Collimated blue-light enhancement in velocity-selective pumped Rb vapour," *J. Phys. At. Mol. Opt. Phys.* **45**(1), 015401 (2012).
24. M. Hennrich, A. Kuhn, and G. Rempe, "Transition from antibunching to bunching in cavity QED," *Phys. Rev. Lett.* **94**(5), 053604 (2005).
25. K. P. Nayak, F. L. Kien, M. Morinaga, and K. Hakuta, "Antibunching and bunching of photons in resonance fluorescence from a few atoms into guided modes of an optical nanofiber," *Phys. Rev. A* **79**(2), 021801 (2009).
26. V. Gomer, B. Ueberholz, S. Knappe, F. Strauch, D. Frese, and D. Meschede, "Decoding the dynamics of a single trapped atom from photon correlations," *Appl. Phys. B* **67**(6), 689–697 (1998).

## 1. Introduction

Since the first experiment on magneto-optical trapping of neutral atoms was reported, the magneto-optical trap (MOT) has become a workhorse for cooling and trapping atoms in the cold-atom physics [1, 2]. Over last twenty years, MOT has been deeply investigated and successfully applied to many fields ranging from precision measurements and atomic clock to single atom trapping and quantum information processing [3–8]. In 2009, a new-configuration MOT has been firstly proposed and demonstrated in experiment [9], which employs optical forces from scattering between excited states replacing one pair of the three pairs of cooling light with a single-photon transition between a ground state and an excited state in a standard MOT. In the case of cesium (Cs) atoms, a pair of the 852.3-nm cooling and trapping laser beams (coupled with  $6S_{1/2} F = 4 - 6P_{3/2} F' = 5$  cycling transition) along the  $z$  (or  $x$ ,  $y$ ) direction in a standard MOT can be replaced with counter-propagating 794.6-nm laser beams coupled with the  $6P_{3/2} F' = 5 - 8S_{1/2} F'' = 4$  excited states transition. This is the so-called two-color MOT, and it can cool and trap atoms on both the red-detuning and blue-detuning sides of the two-photon resonance. This point is remarkably different from the standard MOT which only traps atoms at red single-photon frequency detuning. This kind two-color MOT is also different from the so-called two-color MOT of metastable helium atoms by Tychkov *et al* [10]. Although they cool and trap helium atoms using optical scattering forces between excited states  $2^3S_1 - 3^3P_2$  (389nm) and  $2^3S_1 - 2^3P_2$  (1083nm) cooling transitions, in fact, their MOTs are two standard MOTs with single-photon transition [10]. Just recently, Wang *et al* [11] improved the atom number with "dual color MOT", but their dual color MOT is essentially a standard MOT with different frequency-detuned cooling laser beams [11]. However, the two-color MOT in this paper is based on a ladder-type energy-level configuration which couples the two cooling laser fields (852.3nm plus 794.6nm for Cs atoms  $6S - 6P - 8S$  transitions), so quantum coherence should be fully considered in future. For example, It is also possible to directly generate twin optical beams (or correlated photon pairs) in the two-color MOT based on the four-wave-mixing process in a diamond-type atomic system [12, 13]. The two-color MOT can be used to detect fluorescence signal of the trapped atoms without background on the basis of the ladder-type atomic system, too. In a word, the two-color MOT, as a new method of trapping neutral atoms, should be paid more attentions on.

We have realized the two-color Cs MOT in which one pair of 852.3-nm cooling beams among the three pairs in a standard MOT is replaced with 794.6-nm cooling beams. We also demonstrated a nondestructive background-free detection of fluorescence signals from the atomic transitions driven by no laser beam with the two-color Cs MOT. This is completely different with the background-free image of the cold cloud in a standard MOT [14, 15]. In

that case an additional laser is needed to excite atoms, and more or less it will heat the trapped atoms. The two-color MOT should be especially useful in single atoms MOT experiment for the observation of weak fluorescence signal from single atoms, and in investigation of the photons statistical characteristics, such as photon anti-bunching, and the transition from the photon anti-bunching for single atoms to the photon bunching for atomic ensemble by controlling the number of trapped atoms via changing the quadrupole magnetic field intensity in two-color MOT.

## 2. Experimental setup

The two-color MOT employs the radiation force due to photon scattering from the transition between excited states to replace that from the transition between ground and excited states in one axis among the three axis ( $x$ ,  $y$ ,  $z$ ) of a standard six-beam MOT, so some of the cooling/trapping and repumping laser beams in the standard six-beam MOT are still needed. In our two-color Cs MOT, the 852.3-nm cooling and trapping laser beams ( $\Omega_{ge}$ ) along  $x$  and  $y$  axes (see Fig. 1) are provided by an extended-cavity diode laser (ECDL 1) with a frequency detuning  $\Delta_p = -10$  MHz related to the  $6S_{1/2} F = 4$  (denoted as  $|g\rangle$ ) -  $6P_{3/2} F' = 5$  (denoted as  $|e\rangle$ ) cycling transition. The ECDL 1 is locked by the polarization spectroscopic locking scheme. The repumping laser beams are provided by ECDL 2, which is locked to the Cs  $6S_{1/2} F = 3$  -  $6P_{3/2} F' = 4$  transition by the conventional saturated absorption spectroscopic (SAS) locking scheme.

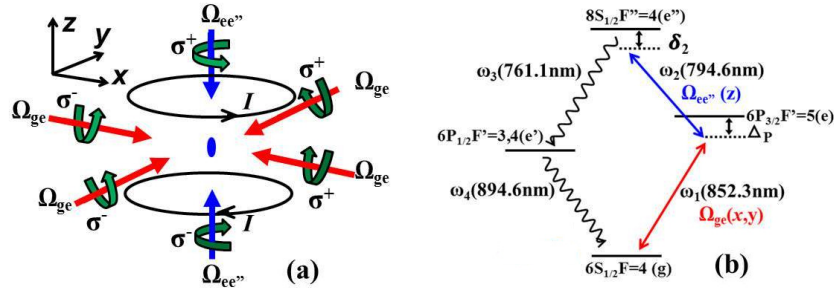


Fig. 1. (a) Two-color MOT configuration. (b) Relevant energy levels of Cs atoms. Keys to figure:  $\sigma^+$ :  $\sigma^+$  circular polarization;  $\sigma^-$ :  $\sigma^-$  circular polarization; I: the current of the anti-Helmholtz coils.

The 794.6-nm cooling and trapping laser beams ( $\Omega_{ee''}$ ) along  $z$  axis (see Fig. 1) are provided by ECDL 3 with a frequency detuning  $\Delta_c$  related to the  $6P_{3/2} F' = 5$  (state  $|e\rangle$ ) -  $8S_{1/2} F'' = 4$  (state  $|e''\rangle$ ) transition, which is locked using an off-resonant double-resonance optical-pumping (DROP) locking scheme [16–18]. The DROP spectrum is based on atomic population transfer from one of the hyperfine manifolds in the ground state to another via the two-photon excitation process to the upper excited state and spontaneous decay through the intermediate states in the ladder-type atomic system. In our laser system for the two-color Cs MOT, as shown in Fig. 2, the ECDL 1 with wavelength 852.3 nm is also used as the probe laser with a frequency detuning  $\Delta'_p$  related to  $|g\rangle$  -  $|e\rangle$  transition independently changed by an acousto-optical modulator (AOM 3). When ECDL 3 with wavelength 794.6-nm as the coupling laser is scanning over  $|e\rangle$  -  $|e''\rangle$  transition, DROP spectrum is obtained. In order to get a narrow linewidth DROP spectrum for locking ECDL 3, the probe and the coupling beams are arranged in counter-propagating configuration. The two laser beams are overlapped in a 5cm-long Cs vapor cell by using a dichroic filter (DF) [16, 17]. When the probe beam is detuned  $\Delta'_p$  from  $|g\rangle$  -  $|e\rangle$  transition, the couple laser is oppositely detuned  $\Delta_c$  from  $|e\rangle$  -  $|e''\rangle$  transition for the requirement of zero two-photon detuning. Due to the Doppler mismatch between the probe and coupling beams, we expect  $\Delta_c = \Delta'_p (\lambda_p/\lambda_c)$ , which is just the frequency interval between the off-resonance DROP peak and the resonant DROP peak ( $\Delta_p =$

$\Delta_C = 0$ , as reference). Finally, the ECDL 3 can be offset locked using an off-resonance DROP spectrum (More detailed locking scheme can be found in our previous work [18]), and its single-photon detuning  $\Delta_C$  can be conveniently controlled from  $-30$  MHz  $\sim +30$  MHz by AOM 3. Furthermore, we can exactly obtain the two-photon detuning  $\delta_2 = -10$  MHz  $+ \Delta_C$  for the cascade  $|g\rangle - |e\rangle - |e''\rangle$  two-photon excitation in the two-color Cs MOT.

An interesting characteristic is that the two-color MOT can efficiently cool and trap atoms at both positive and negative two-photon detunings. With the red two-photon detuning, the cooling/trapping mechanism can be understood by using a two-photon Doppler cooling picture which is similar to that in the standard MOT. With the blue two-photon detuning, the cooling/trapping mechanism may be explained using a two-color polarization gradient cooling picture [9]. In the two-photon cooling process of the two-color Cs MOT, as shown in Fig. 1(b), atoms in state  $|g\rangle$  are optically pumped to state  $|e''\rangle$  via the 852.3-nm and 794.6-nm cooling and trapping laser beams, and then decay back to state  $|g\rangle$  via other intermediate states, for example,  $6P_{1/2}$  ( $7P_{1/2}$  and  $7P_{3/2}$ ), emitting 894.6-nm (459-nm and 456-nm) fluorescence photons, which can be detected by an avalanche photodiode (APD) with a help of proper interference filter (IF) plate. So we can nondestructively detect the trapped atoms via the 894.6-nm fluorescence photons without unwanted background photons scattered from the cooling/trapping and the repumping laser beams with the high-suppression-ratio 894-nm IF plates.

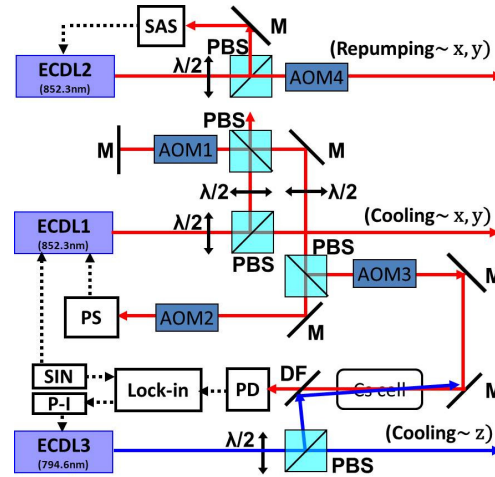


Fig. 2. Our laser system for the two-color Cs MOT. Keys to figure: ECDL: extended-cavity diode laser; SAS: saturated-absorption spectroscopy; PS: polarization spectroscopy; AOM: acousto-optical modulator; Lock-in: lock-in amplifier; P-I: proportion and integration amplifier; SIN: sine-wave signal generator; DF: dichroic filter; M: mirror. PBS: polarization beam splitting cube;  $\lambda/2$ : half-wave plate; PD: photodiode.

### 3. Experimental results and discussions

#### 3.1 Demonstration of the two-color Cs MOT

Among the three pairs of the 852.3-nm cooling/trapping laser beams of the standard six-beam Cs MOT, we replaced one pair of the 852.3-nm cooling laser beams along  $z$  axis (the axis of the anti-Helmholtz coils, see Fig. 1(a)) with the counter-propagating 794.6-nm cooling laser beams which coupled  $|e\rangle - |e''\rangle$  transition. Typical experimental parameters are as follows: the total intensity of the two pairs of the retro-reflected 852.3-nm cooling/trapping beams with a diameter of  $\sim 5$  mm is  $\sim 4 \times 19.9$  mW/cm<sup>2</sup>, and typical single-photon detuning from  $|g\rangle - |e\rangle$  transition is  $\Delta_p = -10$  MHz; the total intensity of the retro-reflected 794.6-nm cooling/trapping beams with a diameter of  $\sim 5$  mm is  $\sim 2 \times 134.6$  mW/cm<sup>2</sup>, and typical two-photon detuning is  $\delta_2 = -14.6$  MHz; the total intensity of the retro-reflected 852.3-nm

repumping laser beams (along the  $x$  and  $y$  directions) with a diameter of  $\sim 5$  mm is  $\sim 4 \times 10.2$  mW/cm<sup>2</sup>; the gradient of the quadrupole magnetic field generated by the anti-Helmholtz coils is 10 Gauss/cm along  $z$  axis, typical pressure inside the metal vacuum chamber is  $\sim 2 \times 10^{-9}$  Torr. The peak fluorescence intensity of the two-color Cs MOT vs the two-photon detuning  $\delta_2$  is plotted in Fig. 3. Inset gives a typical picture of cold cloud in the two-color Cs MOT by using a charge-coupled device (CCD) camera, and its peak fluorescence intensity can be obtained by analyzing the fluorescence picture. Figure 3 clearly shows that two-color Cs MOT can efficiently trap atoms on both the red-detuning and blue-detuning sides of the two-photon resonance when the retro-reflected 794.6-nm cooling/trapping beams along  $z$  axis are intense enough (for example,  $\sim 2 \times 134.6$  mW/cm<sup>2</sup>). When the 794.6-nm cooling/trapping beams are weaker (for example,  $\sim 2 \times 106.4$  mW/cm<sup>2</sup>), the two-color Cs MOT traps atoms mainly at the red two-photon detuning. The above experimental results are very different to that in the standard 852.3-nm Cs MOT, which can only trap atoms at the red single-photon detuning. The highest fluorescence intensity for  $\delta_2 \sim -14.6$  MHz in Fig. 3 corresponds the  $\sim 5 \times 10^6$  trapped atoms in our two-color Cs MOT, which is an order of magnitude smaller than that of the standard 852.3-nm Cs MOT under the similar conditions (likely due to the reduced capture volume and capture velocity for this new-configuration MOT).

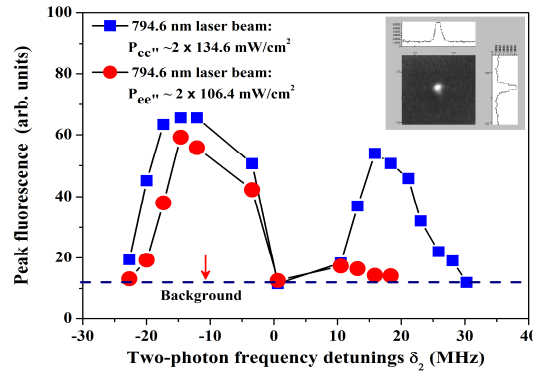


Fig. 3. Peak fluorescence of two-color MOT vs the two-photon frequency detuning  $\delta_2$ . The solid lines are only for guiding eyes, and the dashed line indicates background of the fluorescence signal. Typical MOT parameters: 852.3-nm cooling and trapping laser beams:  $\sim 4 \times 19.9$  mW/cm<sup>2</sup>; 852.3-nm repumping laser beams:  $\sim 4 \times 10.2$  mW/cm<sup>2</sup>; gradient of quadrupole magnetic field:  $\sim 10$  Gauss/cm. The inset shows typical fluorescence image of the cold cloud in our two-color Cs MOT and the intensity distributions along horizontal and vertical directions.

Being different with the  $|g\rangle - |e\rangle$  cooling cycle transition in the standard 852.3-nm Cs MOT, the two-photon  $|g\rangle - |e\rangle - |e''\rangle$  cooling transitions in the two-color Cs MOT is not closed, the atoms populated on state  $|e''\rangle$  in cooling process also may decay back to state  $|g\rangle$  via other intermediate states, for example,  $6P_{1/2}$  (see Fig. 1(b)),  $7P_{1/2}$  and  $7P_{3/2}$  (not shown in Fig. 1(b)), and emit 894.6-nm photons (459-nm and 456-nm blue fluorescence photons) [14]. So it seems intuitively that strong repumping laser should be required. With the optimal experimental parameters based on Fig. 3, we measured the dependence of the peak fluorescence intensity of the trapped atoms in our two-color Cs MOT upon the total intensity of the repumping beams, and the results are shown in Fig. 4. With the increase of the repumping beams' intensity, the peak fluorescence intensity will correspondingly increase, because more and more atoms are captured into the two-color MOT and get saturated at a moderate intensity of the repumping laser  $\sim 10.2$  mW/cm<sup>2</sup>. The stronger the repumping beams keeping the population from pumping into the ground state  $6S_{1/2} F = 3$ , the much efficient the two-photon cooling is. On the other hand, it is just because these intermediate states ( $6P_{1/2}$ ,  $7P_{1/2}$ , and  $7P_{3/2}$ ) exist, they make it possible to nondestructively detect the cold atoms without

background. Also it is possible to directly generate correlated photons pairs based on the four-wave mixing process in the diamond-type atomic system [12, 13] in the two-color Cs MOT.

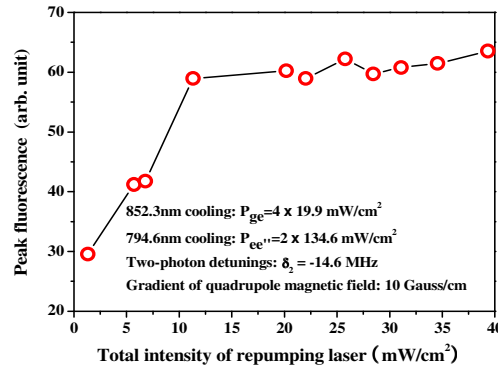


Fig. 4. Peak fluorescence of the two-color Cs MOT vs the total intensity of the repumping laser beams. The solid line is only for guiding eyes.

### 3.2 Background-free fluorescence detection of the trapped atoms in the two-color MOT

Background-free imaging of atoms is an important subject especially for the observation of weak atomic signal, for example, single atoms. In order to apply the two-color MOT to single atom cooling/trapping experiment, the experiments below are performed in another Cs MOT system with a large magnetic gradient (10~300 Gauss/cm). We replace the 852.3-nm standard six-beam Cs MOT along the  $x$  or  $y$  direction with counter-propagating 794.6 nm cooling beams. Here the angle between  $x$  and  $y$  is set to  $60^\circ$  in the horizontal plane which are perpendicular to the  $z$  direction (also the axis of the anti-Helmholtz coils), it is different with the Cs MOT system in Section 3.1. This two-color Cs MOT also can trap atoms on both the red-detuning and blue-detuning sides of the two-photon resonance. Typical experimental parameters are as follows: the total intensity of two pairs of retro-reflected 852.3-nm cooling/trapping beams with a diameter of  $\sim 2.2$  mm along  $x$  (or  $y$ ) and  $z$  axis is  $\sim 189.5$  mW/cm<sup>2</sup>, and typical detuning related to  $|g\rangle - |e\rangle$  transition is  $\Delta_p = -10$  MHz; the total intensity of retro-reflected 794.6-nm cooling/trapping beams with a diameter of  $\sim 2.2$  mm along  $x$  (or  $y$ ) axis is  $\sim 2 \times 226.4$  mW/cm<sup>2</sup>, and typical two-photon detuning is  $\delta_2 = -16.2$  MHz; the total intensity of retro-reflected repumping beams with a diameter of  $\sim 2.2$  mm along  $z$  axis is  $\sim 2 \times 89.5$  mW/cm<sup>2</sup>; the typical gradient of the quadrupole magnetic field along  $z$  axis is set to  $\sim 28$  Gauss/cm; typical pressure inside the cuboid glass vacuum cell is  $\sim 2 \times 10^{-10}$  Torr to decrease the density of Cs atoms in background.

In a standard MOT with single-photon transition cooling, it is difficult to completely distinguish the fluorescence photons of trapped atoms from the background scattering photons of the cooling/trapping and the repumping beams. This will restrict people to get real information of fluorescence photons statistics of a few atoms or single atom [19–21]. In most of experiments people subtracted the contribution of the scattering photons of the cooling/trapping and the repumping beams from the inner walls of vacuum chamber, but it is a post-processing method.

In the two-color Cs MOT, the atomic population transfer from state  $|g\rangle$  to state  $|e''\rangle$  due to excitation of the two-color cooling/trapping beams, and then the cascaded two-photon emissions via  $|e''\rangle - |e'\rangle - |g\rangle$  transitions occur at 761.1 nm and 894.6 nm, as shown in Fig. 1(b). Instead of detection 852.3-nm fluorescence photons, now we can detect 894.6-nm fluorescence photons. Because  $|e'\rangle - |g\rangle$  transition are directly driven by no laser beam, the scattering photons from the cooling/trapping and the repumping beams on the inner walls of



vacuum chamber can be almost completely rejected by using a high-suppression-ratio 894-nm IF plate (Dr. Hugo Anders Optical Laboratories Co., typical peak transmission is  $T \sim 86\%$  at 894.6 nm,  $T \sim 1 \times 10^{-5}$  at 852.3 nm, and  $T < 1 \times 10^{-6}$  at 761 nm and 794.6 nm). Thus we can realize the background-free fluorescence detection of cold atoms in the two-color MOT. One point should be pointed, here the background-free fluorescence detection of trapped atoms in the two-color MOT is very different with the previous method of imaging cold cloud in the standard MOT with one-photon cooling based on a two-stage excitation [14, 15], where it needs additional laser to couple two excited states and will heat cold atoms. Figure 5 shows the 894-nm fluorescence photon counts of cold atoms trapped in our two-color Cs MOT and background photon counts under the conditions of turning off the quadrupole magnetic field and blocking the laser beams along  $x$  ( $y$  or  $z$ ) direction, respectively. The almost same background counts indicate that it is an almost background-free fluorescence detection of cold atoms, and the residual background photon counts mainly came from the dark counts of the APD.

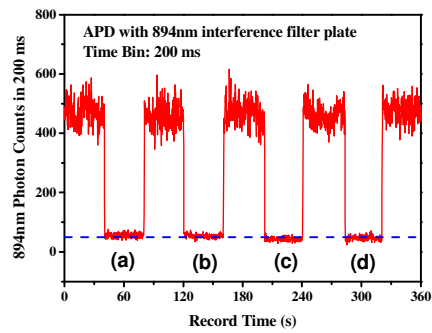


Fig. 5. Typical background-free 894-nm fluorescence photon counting signal of cold atoms in the two-color MOT using APD with help of the 894-nm IF plate. The two-color MOT parameters: the cooling/trapping laser beams along  $\pm x$  for 852.3 nm:  $\sim 2 \times 31.6 \text{ mW/cm}^2$ ;  $\pm y$  for 794.6 nm:  $\sim 2 \times 226.4 \text{ mW/cm}^2$ ;  $\pm z$  for 852.3 nm:  $\sim 2 \times 63.2 \text{ mW/cm}^2$ ; the repumping laser beams along  $\pm z$  for 852.3 nm:  $\sim 2 \times 89.5 \text{ mW/cm}^2$ ; typical gradient of the quadrupole magnetic field:  $\sim 28 \text{ Gauss/cm}$ . (a)–(d) indicate the background 894-nm photon counting levels for the cases of turning off MOT magnetic field (a), blocking the laser beams along  $\pm x$  directions (b), blocking the laser beams along  $\pm y$  directions (c), and blocking the laser beams along  $\pm z$  directions (d), respectively. For detecting 894-nm photons radiated from cold atoms in the two-color Cs MOT, clearly the background 894-nm photon counting levels are almost kept at the same level (dominated by the dark counts of the APD), which is nearly not disturbed by the scattering photons from the 852-nm and 795-nm cooling/trapping laser beams and the 852-nm repumping laser beams.

In order to compare with Fig. 5, we also recorded the 852.3-nm fluorescence photons counts signal of cold atoms in our two-color Cs MOT with the same parameters by using an 852.3-nm IF plate. The results are shown in Fig. 6. It clearly displays that the background photon counts remarkably change when blocking the 852.3-nm laser beams. This is due to the photon scattering of the 852.3-nm cooling/trapping beams (or the repumping beams) from the inner walls of the glass vacuum cell and the background Cs atoms.

We note that the signal magnitude of the 894-nm fluorescence photons is smaller than that of 852-nm fluorescence photons, as shown in Fig. 5 and Fig. 6. One intuitive reason is that the atoms populated on the upper state  $|e\rangle$  decay back to the ground state  $|g\rangle$  by other decay channels, for example, the intermediate  $7P_{1/2}$  and  $7P_{3/2}$  states. The branching ratios are  $\sim 27\%$  for the Cs  $8S_{1/2} - 7P_{3/2}$  transition,  $\sim 14\%$  for the Cs  $8S_{1/2} - 7P_{1/2}$  transition,  $\sim 37\%$  for the Cs  $8S_{1/2} - 6P_{3/2}$  transition, and  $\sim 21\%$  for the Cs  $8S_{1/2} - 6P_{1/2}$  transition [22]. But roughly considering the transmission loss of detection path and quantum efficiency of the APD for 852.3-nm and 894.6-nm photons, the loss from other channels seems impossible to result in

so big difference ( $\sim 10^2$  times) in signal magnitude. Another possible reason is detection direction is not optimized at present stage. We think that there maybe exists the four-wave mixing effect in the two-photon cooling process in the two-color Cs MOT, so the 894.6-nm photons are not isotropic. Furthermore, the repumping laser will greatly enhance the four-wave mixing effect in [23], their experiment is performed in a Rb vapor cell, but the laser system and ladder-type configuration are very similar to that in our two-color MOT. To increase the signal magnitude of 894.6-nm photons, an alternative possible method is to employ the two-color Cs MOT with  $6S_{1/2} - 6P_{3/2} - 7S_{1/2}$  cascade transitions (852 nm plus 1470 nm) for removing the other radiation channels and optimize the detection direction.

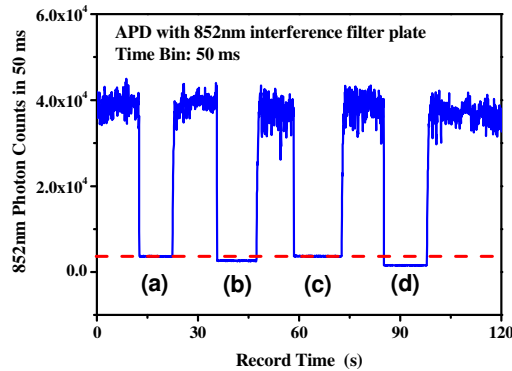


Fig. 6. Typical 852-nm fluorescence photon counting signal of cold atoms in the two-color MOT using APD with help of the 852-nm IF plate. The two-color MOT parameters: the cooling/trapping laser beams along  $\pm x$  for 852.3 nm:  $\sim 2 \times 31.6 \text{ mW/cm}^2$ ;  $\pm y$  for 794.6 nm:  $\sim 2 \times 226.4 \text{ mW/cm}^2$ ;  $\pm z$  for 852.3 nm:  $\sim 2 \times 63.2 \text{ mW/cm}^2$ ; the repumping laser beams along  $\pm z$  for 852.3 nm:  $\sim 2 \times 89.5 \text{ mW/cm}^2$ ; typical gradient of the quadruple magnetic field:  $\sim 28 \text{ Gauss/cm}$ . (a) ~ (d) indicate the background 852-nm photon counting levels for the cases of turning off MOT magnetic field (a), blocking the laser beams along  $\pm x$  directions (b), blocking the laser beams along  $\pm y$  directions (c), and blocking the laser beams along  $\pm z$  directions (d), respectively. For detecting 852-nm photons radiated from cold atoms in the two-color Cs MOT, the background photon counting levels are severely disturbed by the scattering photons from the 852-nm cooling/trapping and the repumping laser beams.

#### 4. Conclusion

We introduced our experimental system, especially presented the controlling of frequency detuning and locking for 794.6-nm cooling/trapping laser between the excited states  $6P_{3/2} - 8S_{1/2}$  transition in detail, which is extremely important for the realization of two-color Cs MOT. We demonstrated the two-color Cs MOT for replacing any pair of 852.3-nm cooling/trapping beams of the three pairs in the standard one-photon six-beam Cs MOT with 794.6-nm cooling/trapping beams which couples the excited states. The two-color MOT can cool and trap atoms on both the red-detuning and blue-detuning sides of the two-photon resonance. Based on the multi-channel ladder-type atomic system, we also measured and analyzed the influence of the repumping laser on the fluorescence intensity of trapped atoms in the two-color Cs MOT, and also demonstrated a nondestructive background-free fluorescence detection of cold atoms by using detection of 894.6-nm fluorescence photons radiated from the two-photon cooling process. The other fluorescence photons at 456 nm, 459 nm, and 761 nm are also feasible.

This two-color Cs MOT scheme possibly can be extended to single-atom Cs MOT for background-free detecting single atoms. It will help us to investigate photons statistical characteristics, such as photon anti-bunching for single atom or a few atoms, and the transition from the photon anti-bunching for single atom to the photon bunching for atomic ensemble [24–26]. In this case we do not need to adopt the post-processing method to subtract



the contribution of the scattering photons of the cooling/trapping and the repumping beams from the inner walls of vacuum chamber and the background Cs atoms.

### **Acknowledgments**

This research work is supported by the National Natural Science Foundation of China (Grant Nos. 11104172, 60978017, and 61078051), the National Major Scientific Research Program of China (Grant No. 2012CB921601), the Project for Excellent Research Team of the National Natural Science Foundation of China (Grant No. 61121064), and the Research Project from Shanxi Scholarship Council of China.